Biochimica et Biophysica Acta 1818 (2012) 2335–2343

Contents lists available at SciVerse ScienceDirect

Biochimica et Biophysica Acta

journal homepage: www.elsevier.com/locate/bbamem

Transfection efficiency boost of cholesterol-containing lipoplexes

Daniela Pozzi [a], Cristina Marchini [b], Francesco Cardarelli [c], Heinz Amenitsch [d], Chiara Garulli [b], Angelo Bifone [c], Giulio Caracciolo [a,*]

[a] Department of Molecular Medicine, "Sapienza" University of Rome, Viale Regina Elena, 324, 00161 Rome, Italy
[b] Department of Bioscience and Biotechnology, University of Camerino, Via Gentile III da Varano, 62032 Camerino (MC), Italy
[c] Center for Nanotechnology Innovation @NEST, Istituto Italiano di Tecnologia, Piazza San Silvestro 12, 56127 Pisa, Italy
[d] Institute of Biophysics and Nanosystems Research, Austrian Academy of Sciences, Schmiedelstrasse 6, A-8042 Graz, Austria

ARTICLE INFO

Article history:
Received 24 March 2012
Received in revised form 8 May 2012
Accepted 14 May 2012
Available online 22 May 2012

Keywords:
Lipoplex
Cholesterol
Transfection efficiency
Membrane fusion
Endosomal escape

ABSTRACT

Most lipid formulations require cholesterol for successful transfection, but the precise reason remains to be more clearly understood. Here, we have studied the effect of cholesterol on the transfection efficiency (TE) of lipoplexes in vitro. Addition of cholesterol to highly effective DC-Chol–DOPE/DNA lipoplexes increases TE, with 40 mol% cholesterol yielding about 10-fold improvement. The transfection mechanisms of cholesterol-containing lipoplexes have been investigated by combining dynamic light scattering, synchrotron small angle X-ray scattering, laser scanning confocal microscopy and transfection efficiency measurements. Our results revealed that cholesterol-containing lipoplexes enter the cells partially by membrane fusion and this mechanism accounts for efficient endosomal escape. We also found evidence that formulations with high cholesterol content are not specifically targeted to metabolic degradation. These studies will contribute to rationally design novel delivery systems with superior transfection efficiency.

1. Introduction

Today, one of the primary objectives of gene therapy is the development of effective, non-toxic gene vectors that can successfully deliver exogenous genetic material into specific cell types, including cancerous cells [1–3]. Viral vectors have a high efficiency of gene delivery, but important concerns have emerged over their safety [4]. This has generated massive interest in non-viral systems that exhibit low safety risks, are capable of carrying large-size molecules and can be produced easily and inexpensively. Among non-viral gene vectors, cationic liposomes (CLs), which are extensively employed as in vitro transfection agents, are emerging as promising candidates for in vivo and ex vivo delivery of nucleic acids for a variety of applications [5–7]. At present, the major disadvantage connected with the use of CL–DNA complexes (lipoplexes) is their low transfection efficiency (TE). This is due to the fact that a multiplicity of intracellular barriers must be overcome to deliver exogenous DNA into the cell nucleus of the host cell and enable its expression [8–11]. Moreover, the internalization route does significantly affect both the intracellular processing and the final fate of lipoplexes. Depending on the mode of cellular uptake, internalization may alternatively lead to lysosomal degradation or digestion, recycling back to the membrane, or delivery to other compartments. Recently, it has been suggested that internalization pathways of lipoplexes are cholesterol-dependent and that cholesterol affects intracellular trafficking of lipoplexes [12,13]. The use of cholesterol in the lipoplex formulation has been shown to enhance transfection both in vitro and in vivo [14,15]. In vitro this could be due, at least in part, to the formation of cholesterol nanodomains in the lipoplex membrane that may play a role either in cellular uptake or in intracellular trafficking [16–18]. In some cell lines, the incorporation of polyethylene glycol into cholesterol domains increased transfection rates, despite the lack of enhancement of cellular uptake [19]. The existence of such cholesterol nanodomains within lipoplex membranes could lead to a general rethinking of current targeting strategies. In vivo, cholesterol is believed to improve transfection by protecting the DNA from degradation by DNAses in the body. In general, cholesterol has been shown to be effective in reducing the binding of serum proteins to lipoplexes [20] thereby improving transfection of DNA, both in vitro and in vivo [21]. Thus, many efforts have been devoted to the synthesis of a series of novel cationic lipids through the systematic substitution of cholesterol derivatives that could greatly enhance the delivery and expression of plasmid DNA [22]. One of the most popular cholesterol-derivative is 3β-[*N*-(*N*′,*N*′-dimethylaminoethane)-carbamoyl]-cholesterol (DC-Chol) [23,24], a cationic molecule that, both alone and combined with other lipids, has been reported to deliver DNA efficiently in most cell lines [25–35]. Beyond the widely used DC-Chol, a huge number of cholesterol-derivatives have been synthesized [36] and successfully used for transfection experiments both in the absence [37] and presence of helper lipids [38]. Cholesterol-based lipids with various

* Corresponding author. Tel.: +39 06 4969 3271; fax: +39 06 490631.
E-mail address: giulio.caracciolo@uniroma1.it (G. Caracciolo).

0005-2736/$ – see front matter © 2012 Elsevier B.V. All rights reserved.
doi:10.1016/j.bbamem.2012.05.017

heterocyclic cationic head groups and linker types were also found to enhance accumulation of nucleic acids in the cells [39].

In summary, most lipid mixtures seem to require cholesterol and/or cholesterol-derivatives for successful transfection, but the precise reason why this happens remains unclear. In this study, we provided novel insights into the transfection mechanisms of cholesterol-containing lipoplexes (CCLs). To this end, we used CLs made of DC-Chol and dioleoylphosphatidylethanolamine (DOPE), one of the most used lipoplex formulations [40,41] and we gradually replaced DOPE molecules by cholesterol. Employing structural studies by dynamic light scattering (DLS) and synchrotron small angle X-ray scattering (SAXS), laser scanning confocal microscopy (LSCM) and transfection efficiency measurements, we were able to elucidate the relation between efficiency and the transfection mechanism of CCLs.

2. Experimental section

2.1. Liposomes preparation

3β-[*N*-(*N*′,*N*′-dimethylaminoethane)-carbamoyl]-cholesterol (DC-Chol) and dioleoylphosphatidylethanolamine (DOPE) were purchased from Avanti Polar Lipids (Alabaster, AL) and used without further purification. Cholesterol was purchased in powder form from Sigma-Aldrich (St. Louis, MO). All mixtures were prepared at molar fractions of cationic lipid in the bilayer $X_{DC\text{-}Chol}=0.5$ and at molar fractions of neutral lipid in the bilayer $X_{DOPE}+X_{Chol}=0.5$, but gradually replacing DOPE molecules with cholesterol molecules. Five different mixtures were prepared with increasing molar fractions of cholesterol ($X_{Chol}=0$, 0.125, 0.25, 0.375, 0.5). Each mixture was dissolved in chloroform and the solvent was evaporated under vacuum for at least 24 h. The obtained lipid films were hydrated with the appropriate amount of Tris–HCl buffer solution (10^{-2} M, pH 7.4) to achieve the desired final concentration (1 mg ml^{-1} for all the experiments except for SAXS experiments where it was 10 mg ml^{-1}).

2.2. Lipoplex preparation

For transfection experiments, plasmid DNA (pGL3 which codifies for firefly luciferase; Promega, Madison, WI) was employed. For SAXS experiments, calf thymus DNA (Sigma-Aldrich, St. Louis, MO) was used. For confocal fluorescence microscopy experiments, Cy5-labeled 2.7-kbp plasmid DNA (Mirus Bio Corporation, Madison, WI) was used. By mixing adequate amounts of the DNA solutions to suitable volumes of liposome dispersions, self-assembled lipoplexes were obtained. For size and ζ-potential measurements samples were prepared at seven cationic lipid/DNA charge ratio (mol/mol), that is, $\rho=$ (cationic lipid (by mole)/DNA base) = 0.25, 0.4, 0.7, 1, 2, 3, 4. On the basis of size and ζ-potential results, all the other experiments were performed at $\rho=3$.

2.3. Size and ζ-potential

Size and size distribution of liposomes and lipoplexes were measured at 25 °C by a Malvern NanoZetaSizer spectrometer equipped with a 5 mW HeNe laser (wavelength $\lambda=632.8$ nm) and a digital logarithmic correlator. The normalized intensity autocorrelation functions were detected at 90° and analyzed by using the CONTIN method, which analyzes the autocorrelation function through an inverse Laplace transform [42,43] in order to obtain the distribution of the diffusion coefficient D of the particles. This coefficient is converted into an effective hydrodynamic radius R_H by using the Stokes–Einstein relationship $R_H=K_BT/(6\pi\eta D)$, where K_BT is the thermal energy and η the solvent viscosity. Our clusters invariably show a size distribution, and the values of the radii reported here correspond to the so-called "intensity weighted" average [44]. The electrophoretic mobility measurements were carried out by means of the laser Doppler electrophoresis technique, the same apparatus used for size measurements. The mobility u was converted into the ζ-potential using the Smoluchowski relation $\zeta=u\eta/\varepsilon$, where η and ε are the viscosity and the permittivity of the solvent phase, respectively.

2.4. Transfection efficiency experiments

Cell lines were cultured in Dulbecco's modified Eagle's medium (DMEM) with Glutamax-1 (Invitrogen, Carlsbad, CA, USA) supplemented with 1% penicillin–streptomycin (Invitrogen) and 10% fetal bovine serum (Invitrogen) at 37 °C and 5% CO_2 atmosphere, splitting the cells every 2–4 days to maintain monolayer coverage. For luminescence analysis, Chinese hamster ovary (CHO) cells were transfected with pGL3 control plasmid (Promega, Fitchburg, WI, USA). In order to investigate the temperature-dependence of lipoplex uptake, CHO cells were transfected with lipoplexes at either 37 or 4 °C. The day before transfection, cells were seeded in 24-well plates (150,000 cells per well) using medium without antibiotics. Cells were incubated until they were 75–80% confluent, which generally took 18–24 h. For TE experiments, lipoplexes were prepared in Optimem (Invitrogen) by mixing for each well of 24-well plates 0.5 μg of plasmid with 5 μl of sonicated lipid dispersions (1 mg ml^{-1}). Complexes were left for 20 min at room temperature before adding them to the cells. On the day of transfection, the growth medium was replaced with 400 μl of Optimem and the cells were incubated for 30 min at either 37 or 4 °C (keeping the well plates containing cells on ice), before adding 100 μl of lipoplexes in Optimem. Cells were incubated at either 37 or 4 °C for an additional 4 h to permit transient transfection. Finally, to avoid internalization of complexes that could remain bound to the cell surface after medium replacement, the cells were extensively washed 3× with phosphate buffered saline (PBS) at the corresponding temperatures (preheated at 37 °C or precooled at 4 °C) before DMEM medium supplemented with 10% fetal bovine serum at 37 °C was added. In experiments where methyl-β-cyclodextrin (500 μM) was used, cells were pretreated for 30 min prior to addition of lipoplexes and incubated during transfection (4 h) with this cholesterol-depleting agent. After 48 h, cells were analyzed for luciferase expression using Luciferase Assay System from Promega. Briefly, cells were washed in PBS and harvested in 200 μl 1× reporter lysis buffer (Promega). Of the cell suspension, 20 μl was diluted in 100 μl luciferase reaction buffer (Promega) and the luminescence was measured 10 s using a Berthold AutoLumat luminometer LB-953 (Berthold, Bad Wildbad, Germany). Results were expressed as relative light units per mg of cell proteins as determined by Bio-Rad Protein Assay Dye Reagent (Bio-Rad, Hercules, CA). Each condition was performed in quadruple and repeated three times.

2.5. Synchrotron small angle X-ray scattering

SAXS measurements were performed at the Austrian SAXS station of the synchrotron light source ELETTRA (Trieste, Italy) [45]. SAXS patterns were recorded with gas detectors based on the delay line principle covering the q-ranges from $q_{min}=0.04$ Å^{-1} to $q_{max}=0.5$ Å^{-1} with a resolution of 5×10^{-4} Å^{-1} (fwhm). The angular calibration of the detectors was performed with silver behenate powder (d-spacing of 58.38 Å). The data have been normalized for variations of the primary beam intensity, corrected for the detector efficiency, and the background has been subtracted. Exposure times were typically 300 s. No evidence of radiation damage was observed in the X-ray diffraction patterns. The sample was held in a 1 mm glass capillary (Hilgenberg, Malsfeld, Germany) and the measurements were performed at 25 °C with a precision of 0.1 °C.

2.6. Cell culture, transfection, and colocalization assays

CHO-K1 were purchased from American Type Culture Collection (CCL-61 ATCC) and were grown in Ham's F12K medium supplemented with 10% of fetal Bovine Serum at 37 °C and in 5% CO_2. For transfection experiments, lipoplexes were prepared in PBS (Invitrogen) by mixing 1 μl of Cy3-labeled DNA with 10 μl of sonicated lipid dispersions. These complexes were left for 20 min at room temperature before adding them to the cells. In order to identify the endocytic vesicles involved in lipoplex internalization, we performed colocalization assays in living cells. CHO-K1 cells were coincubated with lipoplexes and different endocytic fluorescent markers: 1 mg/ml 70 kDa dextran-fluorescein isothiocyanate (FITC) conjugate at 37 °C for 30 min to label macropinosomes, 50 mM Lysosensor for 30 min to label lysosomes, 2 μg/ml transferrin-Alexa488 conjugate for 30 min to label recycling and sorting endosomes. Transfection of Caveolin-E^1GFP^{18} was carried out using lipofectamine reagent (Invitrogen) according to the manufacturer's instruction. Colocalization of green and red signals was analyzed by means of the Pearson's coefficient (*Rr*) using the "colocalization finder" plugin of the ImageJ software (NIH Image; http://rsbweb.nih.gov/ij/) [46].

2.7. Laser scanning confocal microscopy experiments

Laser scanning confocal microscopy (LSCM) experiments were performed with the Olympus Fluoview 1000 (Olympus, Melville, NY) confocal microscope interfaced with a 405 nm diode laser, a 488 nm Argon laser, and 543 nm helium-neon laser. Glass bottom Petri dishes containing transfected cells were mounted in a temperature-controlled chamber at 37 °C and 5% CO_2 and viewed with a 60×1.25 numerical aperture water immersion objective. The following collection ranges were adopted: 500–540 nm (EGFP, Alexa488-transferrin and FITC-Dextran70 kDa), 555–655 nm (Cy3), and 460–530 (Lysosensor). Images were collected in sequential mode to eliminate emission cross talk between the various dyes.

3. Results

3.1. Size and ζ-potential

CLs used in the present study were found to be positively charged ($\zeta_P \approx 60$ mV) with a mean radius, $60\ nm \leq R_H \leq 70\ nm$ (Table 1). Effective formulations must be positively charged with the lowest colloidal dimensions as well. To identify the most appropriate charge ratio for transfection, size and ζ-potential measurements of lipoplexes were determined. In Fig. 1 the hydrodynamic radius, R_H, (panel A) and the ζ-potential, ζ_P, (panel B) of DC-Chol–DOPE–cholesterol/DNA lipoplexes with increasing molar fractions of cholesterol ($X_{Chol}=0$, 0.125, 0.25, 0.375, 0.5) are plotted against the cationic lipid/DNA charge ratio. As can be seen in Fig. 1 (panel A), with the increase of ρ, complex formation starts and the size of the complexes gradually increases until a maximum is reached (at $\rho \sim 1$). Further increase of the lipid content ($\rho > 1$) determines the formation of decreasing-size complexes until a plateau is reached (re-entrant condensation) [47,48]. Fig. 1 (panel B) also shows the charge inversion effect, documented by the ζ-potential values whose sign changes around $\rho \sim 1$, differentiating negative and positively charged aggregates. A sigmoidal curve, similar to that previously found for other lipoplexes can be observed [40]. This trend suggests the existence of three different ζ-potential regions: (i) the region where the net charge of lipoplexes is negative and almost constant at about −50 mV; (ii) the region where the inversion of ζ-potential sign takes place (around $\rho \sim 1$); and (iii) the region where the net charge of the lipoplexes is positive. The results reported in Fig. 1 confirm that the iso-neutrality is reached around $\rho \sim 1$, where complexes exhibited the largest colloidal dimensions. Our results are in good agreement with previous studies showing that lipoplexes show a neutral charge at $\rho \sim 1$ [49]. Lipoplexes at $\rho = 3$ were finally chosen because all of them exhibited positive charge (~40 mV) as well as the lowest colloidal dimensions ($R_H \leq 130$ nm) and the lowest polydispersity index (pdi ~ 0.2).

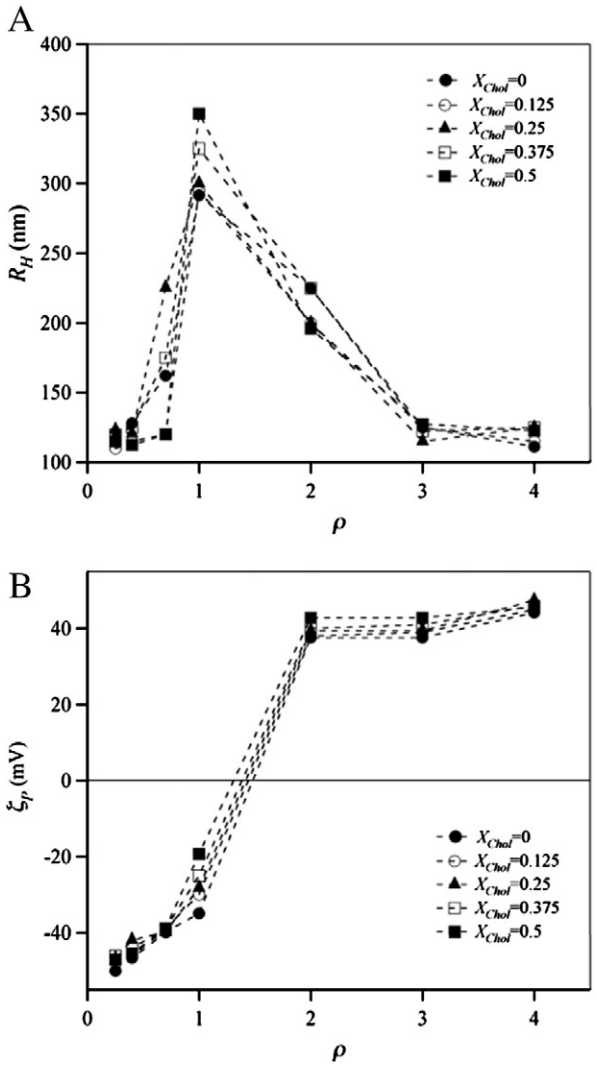

Fig. 1. (A) Hydrodynamic radius, R_H, and (B) zeta potential, ζ_P, of DC-Chol–DOPE–cholesterol/DNA lipoplexes with increasing molar fractions of cholesterol ($X_{Chol}=0$, 0.125, 0.25, 0.375, 0.5) as a function of the cationic lipid/DNA charge ratio, ρ.

Table 1
Hydrodynamic radius, R_H and zeta potential, ζ_P, of DC-Chol–DOPE–cholesterol liposomes with increasing molar fractions of cholesterol ($X_{Chol}=0$, 0.125, 0.25, 0.375, 0.5).

X_{Chol}	R_H (nm)	ζ_P (mV)
0	60 ± 2	58.4 ± 0.3
0.125	67 ± 4	60.1 ± 0.5
0.25	70 ± 3	62.6 ± 0.4
0.375	62 ± 5	64.0 ± 0.4
0.5	65 ± 3	64.7 ± 0.6

3.2. Transfection efficiency

Fig. 2 shows the transfection efficiency of DC-Chol–DOPE–cholesterol/DNA lipoplexes ($\rho = 3$) at five molar fractions of neutral cholesterol in the lipid bilayer ($X_{Chol}=0$, 0.125, 0.25, 0.375, 0.5). We held the charge of the system constant by keeping the DC-Chol content complexes unchanged ($X_{DC\text{-}Chol}=0.5$), and gradually replaced

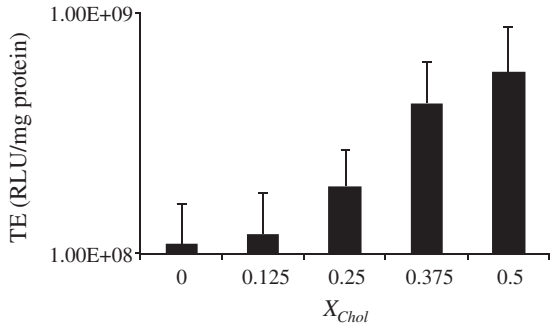

Fig. 2. Transfection efficiency (TE) in RLU per mg of cellular proteins of DC-Chol–DOPE–cholesterol/DNA lipoplexes as a function of increasing molar fractions of cholesterol (X_{Chol} = 0, 0.125, 0.25, 0.375, 0.5). TE increases over about one of magnitude with increasing molar fraction of cholesterol.

DOPE molecules by cholesterol molecules. Fig. 2 shows that addition of cholesterol results in a marked enhancement of TE. Indeed, TE of DC-Chol–DOPE/DNA lipoplexes (X_{Chol} = 0) increases by a factor of 5 with the addition of only 12.5 mol% cholesterol (X_{Chol} = 0.125). Further addition of cholesterol continues to increase the TE. In an effort to rationalize the differences in the efficiency shown in Fig. 2, we first studied the phase organization of DC-Chol–DOPE–cholesterol/DNA lipoplexes at the nanoscale. We were particularly interested in whether the nanostructure of lipoplexes might correlate with their TE.

3.3. Nanostructure

To shed light on the increasing profile of TE versus X_{Chol} (Fig. 2), the nanometric structure of DC-Chol-DOPE-cholesterol/DNA complexes was investigated by means of synchrotron SAXS. Fig. 3 (panel A) shows representative SAXS patterns of DC-Chol-DOPE-cholesterol/DNA (X_{Chol} = 0, 0.25, 0.5) at ρ = 3. The sharp periodically spaced peaks at q_{00l} are caused by an alternating lipid bilayer–DNA–monolayer multilamellar structure with periodicity $d = 2\pi/q_{00l}$. The broad peak marked by an arrow results from one-dimensional (1D) ordering of the DNA sandwiched between the lipid bilayers [50,51]. It is usually referred to as "DNA peak" and corresponds to a DNA interhelical spacing $d_{DNA} = 2\pi/q_{DNA}$. Fig. 3 (panels B and C) shows the variation of d and d_{DNA} as a function of the molar fraction of cholesterol, X_{Chol}. As evident, both the d-spacing and the interhelical spacing, d_{DNA}, decrease as cholesterol content increases. The lamellar spacing drops from 68.3 to 62.2 Å as a function of increasing cholesterol content.

A decrease in d_{DNA} from 38 to 31.2 Å with increasing cholesterol content is most likely to be related to diminution of the surface area of cationic lipid membranes [51–53]. This is expected, because the lateral area per molecule of cholesterol ($A_{\text{cholesterol}} \approx 23.5$ Å^2) [54] is

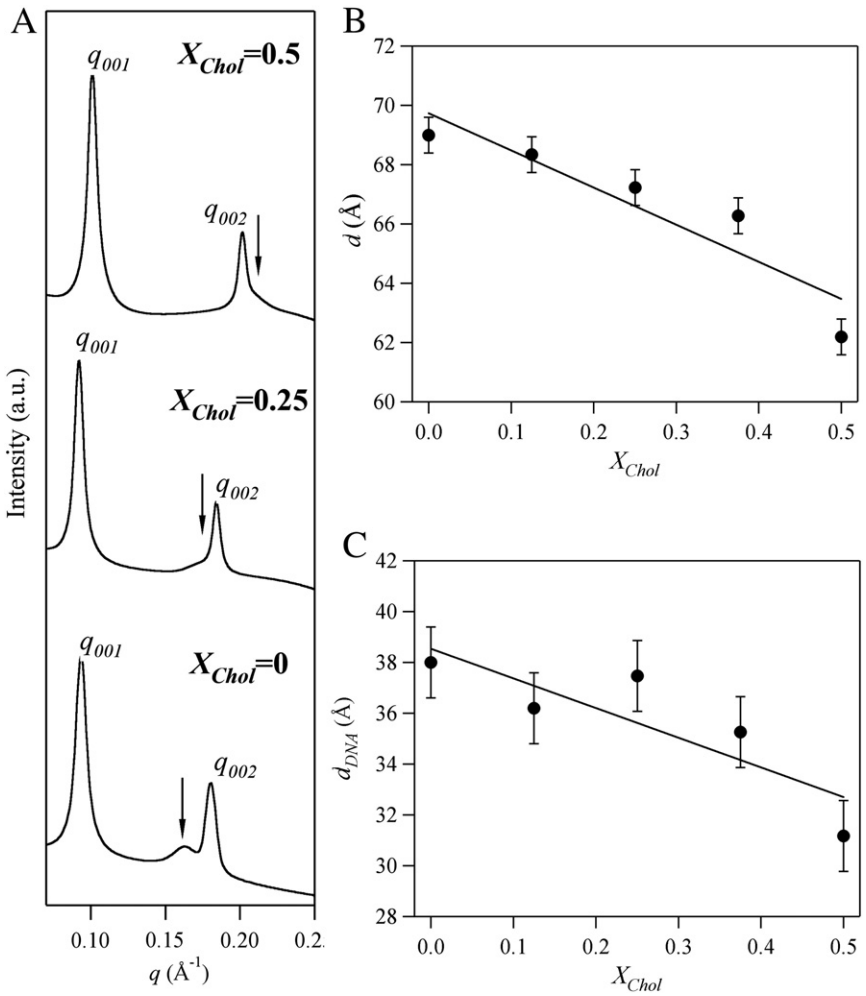

Fig. 3. (A) Representative synchrotron small angle X-ray scattering patterns of DC-Chol–DOPE–cholesterol/DNA lipoplexes. (B) Lamellar spacing, d, of cholesterol-containing lipoplexes obtained from SAXS data. The lamellar spacing decreases from 68.3 to 62.2 Å as a function of increasing cholesterol content. (C) Interhelical distance between DNA molecules embedded within cationic lipid membranes. Solid lines are the best linear fits to data.

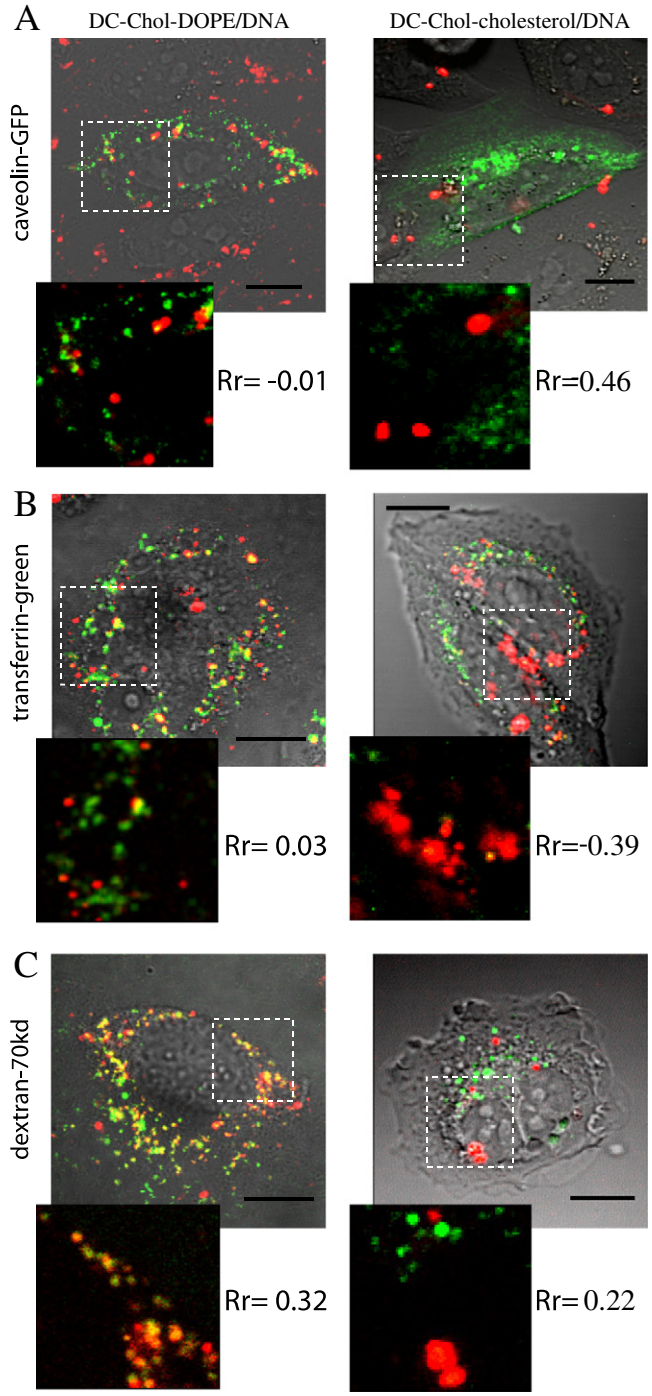

Fig. 4. Colocalization of DC-Chol–DOPE/DNA and DC-Chol–cholesterol/DNA signals (red) with endocytic markers (green). No colocalization was observed with caveolin-E^{1}GFP (caveolar pathway) (A) and Alexa488-transferrin (clathrin pathway) (B) while high correlation (yellow vesicles) was observed with 70 kDa dextran (macropinocytosis) (C). The Pearson's coefficient (Rr) is shown for each measurement. Scale bar = 10 μm.

smaller than that of DOPE ($A_{DOPE} \approx 60$ Å^2) [55], thus reducing the total membrane area. Lastly, we observe that no Bragg peaks arising from cholesterol monohydrate were detected on the SAXS patterns. This finding means that, all over the compositional range ($0 \leq X_{Chol} \leq 0.5$), all cholesterol is incorporated into the lipid bilayer and only a single liquid crystalline phase exists. Previous reports in the literature show that, starting from $X_{Chol} \approx 0.4$, excess cholesterol begins to coexist with lipoplexes as cholesterol monohydrate crystals. Our structural findings therefore suggest that the solubility of cholesterol in DC-Chol-rich membranes is higher than in other cationic lipid membranes used for transfection [17–19,56]. Since the presence of cholesterol-rich nanodomains may affect both the cellular uptake and the intracellular trafficking of lipoplexes [16–18], this finding might be extremely significant for the rational design of lipid gene vectors.

3.4. Uptake mechanism

To clarify the role of cholesterol on the cellular uptake of lipoplexes we used a complementary approach including LSCM and transfection efficiency experiments. To stress possible differences in the uptake mechanism, experiments were performed on DC-Chol–DOPE/DNA and DC-Chol–cholesterol/DNA lipoplexes, as these formulations exhibit the largest difference in the cholesterol content ($X_{Chol} = 0$ and 0.5, respectively). Intracellular trafficking of fluorescently labeled lipoplexes (red) in living cells in the presence of various endocytic markers (green) was investigated by LSCM. The degree of colocalization of green and red fluorescence signals was quantified by means of the Pearson's coefficient (Experimental section). First, a transfection with caveolin-E^{1}GFP was used to label caveolae. At 1 h of treatment with lipoplexes, (Fig. 4, panel A) no clear colocalization of red and green fluorescent signals was found, indicating that both DC-Chol–DOPE/DNA and DC-Chol–cholesterol/DNA lipoplexes were not taken up, at least significantly, through this pathway. Correlation analysis of confocal images confirmed this suggestion (average Pearson's coefficients are reported in Fig. 4).

To investigate if lipoplexes enter cells via the clathrin-coated vesicle-mediated endocytosis pathway, Alexa488-labeled transferrin, marker for clathrin dependent endocytosis, was used. To avoid misleading interpretation experiments were performed 30 min after treatment with lipoplexes. Such reduction in the incubation time is motivated by the fact that macropinosomes may reach the clathrin-positive endosomal checkpoint with time, and might give rise to a misleading increase of the degree of colocalization. Again, as reported in Fig. 4, panel B, the two fluorescence signals remained largely uncolocalized, suggesting that the clathrin pathway is not significantly involved in the cellular uptake of neither DC-Chol–DOPE/DNA and DC-Chol–cholesterol/DNA lipoplexes.

Finally, macropinocytosis was visualized by treating cells with a fluorescently-labeled 70-kDa dextran. Since macropinocytosis is a fluid phase uptake, it is expected to be a slower process. Thus, LSCM experiments were performed after incubating the lipoplexes with cells for varying time periods of 15 min, 30 min, 1 h and 3 h. At t = 3 h we observe that both the lipoplex formulations colocalized with dextran in living cells, although with a difference in the overall amount of correlation between the two signals (Fig. 4, panel C). In detail, despite their higher transfection efficiency, DC-Chol–cholesterol/DNA lipoplexes show a decreased colocalization with the macropinosome marker compared to that of DC-Chol–DOPE/DNA ones ($R_r = 0.11 \pm 0.09$ vs $R_r = 0.39 \pm 0.08$, Table 2). This apparent discrepancy is explained by the presence of large (μm-sized) red patches around several macropinosomes in the case of DC-Chol–cholesterol/DNA lipoplexes (see zoomed detail in Fig. 4, panel C). Besides providing an explanation for the reduction in the colocalization factor, this effect strongly suggests that cholesterol-enriched lipoplexes are capable of efficient and early escape from macropinosomes. At this stage, it is worth noting that similar "escape" patches are also present in the colocalization assays with caveolin-E^{1}GFP and transferring-green, but with the obvious absence of correlation (i.e. absence of contribution of the caveolar and clathrin routes).

Since it has been recently shown that lipoplex macropinocytosis is a cholesterol-sensitive uptake mechanism [57] we asked whether cholesterol depletion could have an effect on the cellular uptake of CCLs. Cholesterol depletion on the plasma membrane by methyl-β-

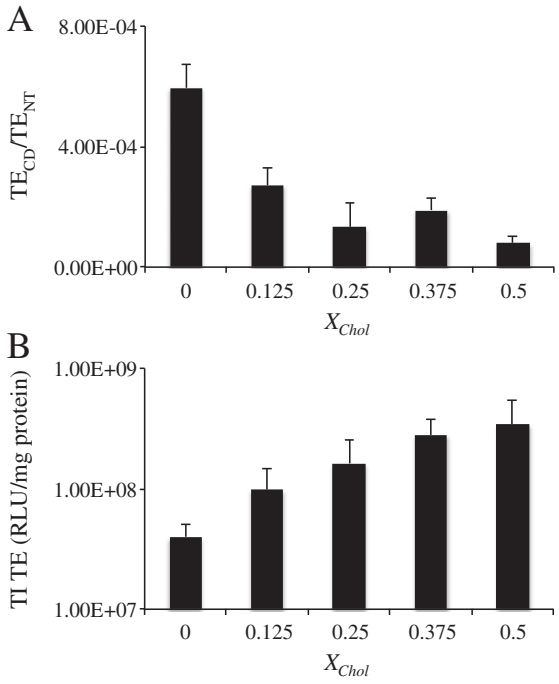

Fig. 5. (A) Reduction in transfection efficiency (TE) of cholesterol-containing lipoplexes expressed by the ratio between the TE measured in cells treated with methyl-β-cyclodextrin, TE_{CD}, and that measured in nontreated cells, TE_{NT}, as a function of increasing molar fractions of cholesterol (X_{Chol} = 0, 0.125, 0.25, 0.375, 0.5). (B) Temperature-independent TE measured at 4 °C in RLU per mg of cellular proteins of DC-Chol–DOPE–cholesterol/DNA lipoplexes as a function of increasing molar fractions of cholesterol (X_{Chol} = 0, 0.125, 0.25, 0.375, 0.5).

cyclodextrin had a dramatic effect on the TE of lipoplexes. Fig. 5 panel A shows the reduction in TE expressed by the ratio between the TE of treated, TE_{CD}, and that nontreated cells, TE_{NT}. Remarkably, the TE_{CD}/TE_{NT} efficiency ratio did directly correlate with the cholesterol content: the higher the cholesterol content, the higher the reduction in TE. These findings indicate a key role of cholesterol in the lipoplex uptake and subsequent trafficking.

As explained above, our fluorescence-based colocalization assays reveal that DC-Chol–cholesterol/DNA lipoplexes (Fig. 4, right panels) have a high propensity to form large intracellular structures, at least part of which is associated with macropinosomes. In this connection it is important to consider that, in addition to endocytosis, several different pathways, probably mediated by direct fusion between lipoplexes and the plasma membrane, have been suggested as alternative routes for the functional delivery of genetic material [58]. Endocytosis is a temperature-dependent (TD) process (it does not take place at 4 °C), while direct transport through the plasma membrane is supposed to be a temperature-independent (TI) process, as it occurs even at low T [59–63]. A common way to probe the existence of TI uptake mechanisms is to perform TE experiments at 4 °C. When cells were transfected at 4 °C, all the lipoplex formulations transfected cells efficiently (Fig. 5, panel B). According to literature, this finding is likely to suggest that CCLs enter cells, at least partially, via a mechanism other than endocytosis. Remarkably, TI-TE monotonically increased with increasing molar fraction of cholesterol, thus suggesting that TI-mechanisms are favored in cholesterol-enriched formulations. In particular, the addition of only 12.5 mol% cholesterol affords a 4-fold raise in the TI-TE factor.

In summary, our findings about the cellular uptake of CCLs can be summarized as follows: CCLs use either (i) a cholesterol-dependent macropinocytosis pathway and (ii) a TI mechanism to enter cells. The latter mechanism does strictly correlate with cholesterol content: specifically, the higher the cholesterol content of lipoplexes, the higher their TI-TE.

Table 2
Pearson's coefficients for lipoplexes colocalization with endocytic markers. The number of cells used for the calculation is reported in parentheses.

	Caveolin	Transferrin	Dextran
DC-Chol–DOPE/DNA	−0.01 ± 0.05 (7)	0.06 ± 0.05 (10)	0.39 ± 0.08 (10)
DC-Chol–cholesterol/DNA	−0.46 ± 0.15 (7)	−0.39 ± 0.07 (7)	0.11 ± 0.09 (13)

3.5. Intracellular final fate

To account for differences in TE, the ultimate intracellular fate of lipoplexes was finally evaluated. To this end, colocalization of DC-Chol–DOPE/DNA and DC-Chol–cholesterol/DNA lipoplexes with Lysosensor (lysosome marker, green) was investigated. After 3 h of incubation with DC-Chol–DOPE/DNA lipoplexes, minor colocalization of red and green signals was observed, together with detectable lipoplex escape from lysosomes, as testified by the large uncolocalized red patches (Fig. 6). This observation provides a reasonable explanation for their good TE (Fig. 1) [64]. Strikingly, when cells were transfected with DC-Chol–cholesterol/DNA lipoplexes no colocalization with Lysosensor was found. This observation was fully supported by correlation analysis of confocal images. Remarkably, Fig. 6 shows typical morphological changes of DC-Chol–cholesterol/DNA lipoplexes that appear as extremely large structures (typically > 2 μm). Such large structures are

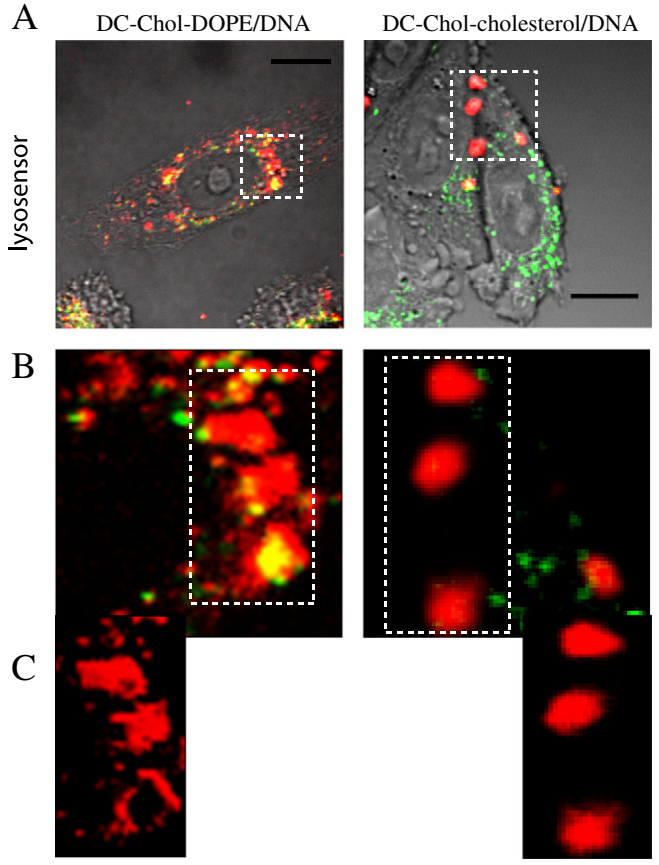

Fig. 6. Colocalization of DC-Chol–DOPE/DNA and DC-Chol–cholesterol/DNA signals (red) with Lysosensor (lysosome marker, green), after 3 h of lipoplex treatment (A). Both the lipoplex formulations are able to avoid lysosomal entrapment (B). When cells are treated with DC-Chol–cholesterol/DNA lipoplexes large structures arise from extensive membrane reorganization (C). Scale bar = 10 μm.

not observed at the early step of lipoplex entry (not reported) and formation could arise from extensive membrane reorganization [65]. The complete absence of colocalization of the DC-Chol–cholesterol/DNA lipoplexes with Lysosensor demonstrates that this formulation is not specifically targeted to metabolic degradation. Together with the lower degree of colocalization with macropinosomes and the observed contribution of a TI mechanism, these data again support the higher transfection efficiency of cholesterol-enriched lipoplexes.

4. Discussion

Previous studies have shown that lipoplexes with high levels of cholesterol and/or cholesterol-derivatives exhibited enhanced transfection [66–70] and resistance to serum-induced aggregation [71,72]. While the involvement of cholesterol in numerous cellular mechanisms and processes is well established, the reason why it should improve the transfection efficiency of lipid gene vectors has not been clarified so far. The rationale for this study was thus to better understand the molecular mechanisms governing the cellular uptake and the final fate of CCLs. This in turn would help to identify critical steps that could be pharmacologic targets for improved transfection. To this end, we used CL formulations made of the cationic lipid DC-Chol, and the neutral lipid DOPE, and we gradually replaced DOPE molecules by cholesterol. It is known that several physical–chemical parameters control lipofection. Among them, lipid/DNA charge ratio, size and zeta-potential can dramatically affect TE. To avoid misleading interpretations, we kept lipid/DNA charge ratio, size and zeta-potential constant. Hence, we performed an accurate preliminary characterization concerning the size and the ζ-potential of the lipid/DNA supramolecular aggregates (Fig. 1). Upon lipoplex formation, both reentrant condensation and charge inversion occurred (Fig. 1). The proper lipoplex formulations for transfection studies were chosen according to the following general considerations: (i) lipoplexes must be positively charged to associate electrostatically with mammalian cells, which contain surface proteoglycans with negatively charged sulfated groups; (ii) excess amount of cationic lipid (i.e. large ρ values) is detrimental in terms of lipid toxicity to the cells; and (iii) homogeneous small-size complexes are better internalized and processed by cells. As a result, lipoplexes at $\rho = 3$ were selected because all of them exhibited a positive charge (~40 mV) as well as the lowest colloidal dimensions ($R_H \leq 130$ nm) and the lowest polydispersity index (pdi ~ 0.2). Recent studies clearly show that, in a given cell line, internalization and uptake kinetics of nanoparticles are highly size-dependent [73]. Thus, since size of CCLs remain almost unchanged with increasing molar fractions of cholesterol, this parameter could not be taken into account to explain differences in their cellular uptake, final fate and TE.

When lipoplexes were given to cells, all the formulations yielded high TE (Fig. 2). Remarkably, a clear TE enhancement can be observed for $0 < X_{Chol} <$ and 0.375, and no further TE increase is clearly seen for $X_{Chol} > 0.375$. This result is in good agreement with previous findings showing that TE of CCLs raises up to $X_{Chol} \approx 0.4$ [56]. In an effort to rationalize the differences in the efficiency shown in Fig. 2, we first studied the phase organization of DC-Chol–DOPE–cholesterol/DNA lipoplexes. We were particularly interested in whether the nanostructure of lipoplexes might correlate with their TE. In fact, one possible explanation for the increase in TE could be a phase transition, promoted by cholesterol, toward a non-lamellar most transfecting phase [74–77]. SAXS experiments showed that lipoplexes remained lamellar with increasing cholesterol content and no phase transition occurred (Fig. 3, panel A). However, we observed that the interlamellar periodicity d decreased more than 6 Å with increasing X_{Chol} (Fig. 3, panel A), due to the reduced hydration layer of cholesterol molecules [56]. At small intermembrane distances, the presence of a strong repulsive force commonly known as the "hydration force" represents a major barrier for membrane interaction and fusion. This repulsive interaction between lipid membranes is probably the result of lipid molecules perturbing the water structure close to the lipid–water interface. It has also been suggested that the hydration force is due to a partial charge transfer between the lipid polar headgroups and the water molecules resulting in a sort of "chemical hydration" of the bilayer surface. When DOPE gets replaced by cholesterol, the average hydration repulsion layer of the membrane is reduced leading to a reduced hydration repulsion and thus enhanced fusion of the cationic membranes of lipoplexes with the anionic cellular membranes [56,78]. In this light, cholesterol-rich lipoplexes are expected to be favored in the interaction with the cellular membranes, thus facilitating fusion-driven cellular uptake and/or endosomal release, depending on the mechanism of entry coming into play. To clarify this point, we investigated the cellular uptake and final fate of lipoplexes. By a combination of imaging and pharmacological approaches we have demonstrated that the main endocytic pathway involved in CCLs' internalization and trafficking is cholesterol-dependent macropinocytosis (Fig. 4). When the final fate of CCLs was investigated, however, no marked colocalization with lysosomes was found (Fig. 6), in keeping with the purported escape ability of both DC-Chol–DOPE/DNA and DC-Chol–cholesterol/DNA formulations. At this stage, by confocal imaging we registered a higher propensity of DC-Chol–cholesterol/DNA to form large intracellular structures or plaques compared to DC-Chol–DOPE/DNA. This is testified by a detectable reduction in the colocalization of lipoplexes with macropinosomes at higher cholesterol concentrations. This in turn suggests either an early release from vesicles and/or the concomitant existence of a vesicle-independent process.

Notably, TE experiments performed at 4 °C, where endocytosis does not take place, demonstrated the presence of a TI pathway that is progressively favored by increasing amounts of cholesterol in the lipoplex formulation (Fig. 5, panel B). Even though the lipoplex–cellular membrane interaction accounting for the TI transfection is presently unknown, it is most likely controlled by lipid mixing between lipoplex and cellular lipids. Resina et al. assumed that the TI-TE of Neutraplex lipoplexes [63], which are second generation highly-effective gene vector systems, might be due to lipid mixing and concomitant membrane fusion. Indeed, lipids mix quickly during individual hemifusion/fusion events and lipid mixing is usually taken as an indication of membrane fusion. This suggestion is further supported by a recent study by Ming et al. who showed that oligonucleotides delivered by lipoplexes enter the cells partially by membrane fusion [79]. Given the high TI-TE of cholesterol-containing lipoplexes, it is conceivable to hypothesize that a mechanism of direct fusion between lipoplexes and cellular membranes plays a role also at higher temperature, thus explaining the transfection efficiency boost observed at 37 °C (Fig. 1).

Taken together, our results put forth the concept that cholesterol can act as promoter of lipoplex fusion with both the plasma and the endosomal membranes. This idea is further strengthened by several results present in literature, as discussed in the following. First, it has been demonstrated that cholesterol is able to promote and stabilize local bilayer negative curvature (bending), a crucial step during the membrane fusion process [79,80]. Membrane fusion proceeds by means of intermediates in which the proximal leaflets of the fusing membranes are merged, whereas the distal leaflets are separate (fusion stalk), followed by the opening of small aqueous "fusion pores" that might be determinant for the cytosolic release of the gene payload [81]. Accordingly, it has been recently shown that addition of cholesterol in phospholipid membranes facilitates the formation of bicontinuous cubic phases at physiological temperatures and increases their ability for fusion [82]. The role of cholesterol in promoting membrane fusion has been a matter of frequent investigation in the field of viral vector-mediated gene transfer. It is worth mentioning that several enveloped viruses rely on the presence of cholesterol to promote their own entry into cells [83–85]. Indeed, cholesterol depletion has been found to inhibit fusion of vaccinia virus (VACV) with plasma membrane [86]. Also, successful infection by influenza virus

requires that the envelope spike protein, hemagglutinin (HA), catalyzes fusion between the viral envelope and the intracellular endosomal membrane of the target cell, thus creating a pore large enough to release the viral genome [86]. While the association of HA with cholesterol-rich domains does explain why the virus infectivity is inhibited by cholesterol depletion, the role of cholesterol seems to be even more important than this. Cholesterol acts at two stages in membrane fusion: (1) early, prior to fusion pore opening, it promotes the formation and growth of the contact sites needed for lipid mixing and (2) late, it helps to expand the fusion pore, thereby increasing the efficiency of fusion. In light of these findings, we are prompted to conclude that, in our system, cholesterol facilitates lipoplex–cellular lipid mixing leading to membrane fusion at the level of both the plasma and endosomal membranes. Very similar results have been recently achieved with pyridinium-based lipoplexes that promote transient permeabilization of cells and allow deep tissue penetration [87,88]. As a matter of fact, our results suggest that the role of cholesterol on lipofection resembles that played in the early steps of cellular infection by viruses.

5. Conclusions

In conclusion, we have shown that CCLs use either (i) a cholesterol-dependent macropinocytosis pathway and (ii) a TI mechanism to enter cells. The latter mechanism is strictly related with cholesterol content: the higher the cholesterol content of lipoplexes, the higher their TI-TE. We also found evidence that formulations with high cholesterol content are not specifically targeted to metabolic degradation. This mechanism of action of CCLs should be considered for the rational design of novel delivery systems with superior transfection efficiency. It has recently been shown that nanoparticle uptake and cellular processing are both affected by the cell cycle [89] that is, in turn, largely regulated by cholesterol. Furthermore, nanoparticles of the same type are differently uptaken in different cell types [90]. Experiments aimed at evaluating the role of cell cycle and type on the uptake and final fate of cholesterol-containing lipoplexes are currently in progress in our laboratories.

References

[1] M. Cavazzana-Calvo, S. Hacein-Bey, G. de Saint Basile, F. Gross, E. Yvon, P. Nusbaum, F. Selz, C. Hue, S. Certain, J.L. Casanova, P. Bousso, F.L. Deist, A. Fischer, Gene therapy of human severe combined immunodeficiency (SCID)-X1 disease, Science 288 (2000) 669–672.
[2] E. Marshall, Gene therapy on trial, Science 288 (2002) 951–952.
[3] C.R. Dass, Lipoplex-mediated delivery of nucleic acids: factors affecting in vivo transfection, J. Mol. Med. 82 (2004) 579–591.
[4] S. Hacein-Bey-Abina, C. von Kalle, M. Schmidt, F. Le Deist, A serious adverse event after successful gene therapy for X-linked severe combined immunodeficiency, N. Engl. J. Med. 348 (2003) 255–256.
[5] M. Mével, C. Neveu, C. Gonçalves, J.J. Yaouanc, C. Pichon, P.A. Jaffrès, P. Midoux, Novel neutral imidazole-lipophosphoramides for transfection assays, Chem. Commun. 21 (2008) 3124–3126.
[6] P. Midoux, C. Pichon, J.J. Yaouanc, P.A. Jaffres, Chemical vectors for gene delivery: a current review on polymers, peptides and lipids containing histidine or imidazole as nucleic acids carriers, Br. J. Pharmacol. 157 (2009) 166–178.
[7] Guo, L. Huang, Recent advances in nonviral vectors for gene delivery, Acc. Chem. Res. DOI: http://dx.doi.org/10.1021/ar200151m.
[8] I.S. Zuhorn, D. Hoekstra, On the mechanism of cationic amphiphile-mediated transfection. To fuse or not to fuse: is that the question? J. Membr. Biol. 189 (2002) 167–179.
[9] A. Elouahabi, J.M. Ruysschaer, Formation and intracellular trafficking of lipoplexes and polyplexes, Mol. Ther. 11 (2005) 336–347.
[10] L.K. Medina-Kauwe, J. Xie, S. Hamm-Alvarez, Intracellular trafficking of nonviral vectors, Gene Ther. 12 (2005) 1734–1751.
[11] G. Candiani, D. Pezzoli, L. Ciani, R. Chiesa, S. Ristori, Bioreducible liposomes for gene delivery: from the formulation to the mechanism of action, PLoS One 5 (2010) e13430.
[12] I.S. Zuhorn, R. Kalicharan, D. Hoekstra, Lipoplex-mediated transfection of mammalian cells occurs through the cholesterol-dependent clathrin-mediated pathway of endocytosis, J. Biol. Chem. 277 (2002) 18021–18028.
[13] J. Rejman, V. Oberle, I.S. Zuhorn, D. Hoekstra, Size-dependent internalization of particles via the pathways of clathrin- and caveolae-mediated endocytosis, Biochem. J. 377 (2004) 159–169.
[14] K. Crook, B.J. Stevenson, M. Dubouchet, D.J. Porteous, Inclusion of cholesterol in DOTAP transfection complexes increases the delivery of DNA to cells in vitro in the presence of serum, Gene Ther. 5 (1998) 137–143.
[15] A.P. Dabkowska, D.J. Barlow, A.V. Hughes, R.A. Campbell, P.J. Quinn, M.J. Lawrence, The effect of neutral helper lipids on the structure of cationic lipid monolayers, J. R. Soc. Interface 9 (2012) 548–561.
[16] X.B. Zhao, N. Muthusamy, J.C. Byrd, R.J. Lee, Cholesterol as a bilayer anchor for PEGylation and targeting ligand in folate-receptor-targeted liposomes, J. Pharm. Sci. 96 (2007) 2424–2435.
[17] L. Xu, T.J. Anchordoquy, Cholesterol domains in cationic lipid/DNA complexes improve transfection, Biochim. Biophys. Acta 1778 (2008) 2177–2181.
[18] L. Xu, T.J. Anchordoquy, Effect of cholesterol nanodomains on the targeting of lipid-based gene delivery in cultured cells, Mol. Pharm. 7 (2010) 1311–1317.
[19] L. Xu, M.F. Wempe, T.J. Anchordoquy, The effect of cholesterol domains on PEGylated liposomal gene delivery in vitro, Ther. Deliv. 2 (2011) 451–460.
[20] H. Faneca, S. Simões, M.C.P. de Lima, Evaluation of lipid-based reagents to mediate intracellular gene delivery, Biochim. Biophys. Acta 1567 (2002) 23–33.
[21] F. Koster, D. Finas, C. Schulz, C. Hauser, K. Diedrich, R. Felberbaum, Additive effect of steroids and cholesterol on the liposomal transfection of the breast cancer cell line T-47D, Int. J. Mol. Med. 14 (2004) 769–772.
[22] H. Gao, K.M. Hui, Synthesis of a novel series of cationic lipids that can act as efficient gene delivery vehicles through systematic heterocyclic substitution of cholesterol derivatives, Gene Ther. 8 (2001) 855–863.
[23] X. Gao, L. Huang, A novel cationic liposome reagent for efficient transfection of mammalian cells, Biochem. Biophys. Res. Commun. 179 (1991) 280–285.
[24] S. Li, X. Gao, K. Son, F. Sorgi, H. Hofland, L. Huang, DC-Chol lipid system in gene transfer, J. Control. Release 39 (1996) 373–381.
[25] G. Caracciolo, D. Pozzi, R. Caminiti, H. Amenitsch, Lipid mixing upon deoxyribonucleic acid-induced liposomes fusion investigated by synchrotron small-angle X-ray scattering, Appl. Phys. Lett. 87 (2005) 133901.
[26] D. Pozzi, H. Amenitsch, R. Caminiti, G. Caracciolo, How lipid hydration and temperature affect the structure of DC-Chol–DOPE/DNA lipoplexes, Chem. Phys. Lett. 422 (2005) 439–445.
[27] G. Caracciolo, R. Caminiti, Do DC-Chol/DOPE–DNA complexes really form an inverted hexagonal phase? Chem. Phys. Lett. 411 (2005) 327–332.
[28] G. Caracciolo, D. Pozzi, H. Amenitsch, R. Caminiti, Interaction of lipoplexes with anionic lipids resulting in DNA release is a two-stage process, Langmuir 23 (2007) 8713–8717.
[29] G. Caracciolo, D. Pozzi, R. Caminiti, C. Marchini, M. Montani, A. Amici, H. Amenitsch, Transfection efficiency boost by designer multicomponent lipoplexes, Biochim. Biophys. Acta 1768 (2007) 2280–2292.
[30] G. Caracciolo, D. Pozzi, R. Caminiti, C. Marchini, M. Montani, A. Amici, H. Amenitsch, Enhanced transfection efficiency of multicomponent lipoplexes in the regime of optimal membrane charge density, J. Phys. Chem. B 112 (2008) 11298–11304.
[31] G. Caracciolo, R. Caminiti, M.A. Digman, E. Gratton, S. Sanchez, Efficient escape from endosomes determines the superior efficiency of multicomponent lipoplexes, J. Phys. Chem. B 113 (2009) 4995–4997.
[32] C. Marchini, D. Pozzi, C. Alfonsi, M. Montani, A. Amici, H. Amenitsch, G. Caracciolo, Coupling between lipoplex and plasma membrane lipid composition: a trojan horse for cell entry? Langmuir 26 (2010) 13867–13873.
[33] . G. Caracciolo, L. Callipo, S. Candeloro De Sanctis, C. Cavaliere, D. Pozzi, A. Laganà, Surface adsorption of protein corona controls the cell internalization mechanism of DC-Chol–DOPE/DNA lipoplexes in serum, Biochim. Biophys. Acta 1798 (2010) 536–543.
[34] G. Caracciolo, D. Pozzi, S. Candeloro De Sanctis, A.L. Capriotti, G. Caruso, R. Samperi, A. Laganà, Effect of membrane charge density on the protein corona of cationic liposomes: interplay between cationic charge and surface area, Appl. Phys. Lett. 99 (2011) 033702.
[35] C. Marchini, D. Pozzi, M. Montani, C. Alfonsi, A. Amici, S. Candeloro De Sanctis, M.A. Digman, S. Sanchez, E. Gratton, H. Amenitsch, A. Fabbretti, C.O. Gualerzi, G. Caracciolo, Role of temperature-independent lipoplex–cell membrane interactions in the efficiency boost of multicomponent lipoplexes, Cancer Gene Ther. 18 (2011) 543–552.
[36] J. Biswas, S.K. Mishra, P. Kondaiah, S. Bhattacharya, Syntheses, transfection efficacy and cell toxicity properties of novel cholesterol-based gemini lipids having hydroxyethyl head group, Org. Biomol. Chem. 9 (2011) 4600–4613.
[37] M.D. Kearns, A.M. Donkor, M. Savva, Structure–transfection activity studies of novel cationic cholesterol-based amphiphiles, Mol. Pharm. 5 (2007) 128–139.
[38] M.D. Kearns, Y.N. Patel, M. Savva, Physicochemical characteristics associated with transfection of cationic cholesterol-based gene delivery vectors in the presence of DOPE, Chem. Phys. Lipids 163 (2010) 755–764.
[39] D.A. Medvedeva, M.A. Maslov, R.N. Serikov, N.G. Morozova, G.A. Serebrenikova, D.V. Sheglov, A.V. Latyshev, V.V. Vlassov, M.A. Zenkova, Novel cholesterol-based cationic lipids for gene delivery, J. Med. Chem. 52 (2009) 6558–6568.
[40] L. Ciani, A. Casini, C. Gabbiani, S. Ristori, L. Messori, G. Martini, DOTAP/DOPE and DC-Chol/DOPE lipoplexes for gene delivery studied by circular dichroism and other biophysical techniques, Biophys. Chem. 127 (2007) 213–220.
[41] Y. Zhang, H. Li, J. Sun, J. Gao, W. Liu, B. Li, Y. Guo, J. Chen, DC-Chol/DOPE cationic liposomes: a comparative study of the influence factors on plasmid pDNA and siRNA gene delivery, Int. J. Pharm. 390 (2010) 198–207.
[42] S.W. Provencher, A constrained regularization method for inverting data represented by linear algebraic or integral equations, Comput. Phys. Commun. 27 (1982) 213–227.
[43] S.W. Provencher, CONTIN: a general purpose constrained regularization program for inverting noisy linear algebraic and integral equations, Comput. Phys. Commun. 27 (1982) 229–242.

[44] B.J. Berne, R. Pecora, Dynamic Light Scattering: With Applications to Chemistry, Biology, and Physics, Dover Publications Inc, New York, 2003.
[45] H. Amenitsch, M. Rappolt, M. Kriechbaum, H. Mio, P. Laggner, S. Bernstorff, First performance assessment of the small-angle X-ray scattering beamline at ELETTRA, J. Synchrotron Radiat. 5 (1998) 506–508.
[46] V. Zinchuk, O. Zinchuk, T. Okada, Quantitative colocalization analysis of multicolor confocal immunofluorescence microscopy images: pushing pixels to explore biological phenomena, Acta Histochem. Cytochem. 40 (2007) 101–111.
[47] S. Zuzzi, C. Cametti, G. Onori, Polyion-induced aggregation of lipidic-coated solid polystyrene spheres: the many facets of complex formation in low-density colloidal suspensions, Langmuir 24 (2008) 6044–6049.
[48] S. Zuzzi, C. Cametti, G. Onori, S. Sennato, S. Tacchi, Polyion-induced cluster formation in different colloidal polyparticle aqueous suspensions, Langmuir 25 (2009) 5910–5917.
[49] A. Rodrıguez-Pulido, F. Ortega, O. Llorca, E. Aicart, E. Junquera, A physicochemical characterization of the interaction between DC-Chol/DOPE cationic liposomes and DNA, J. Phys. Chem. B 112 (2008) 12555–12565.
[50] G. Caracciolo, R. Caminiti, DNA–DNA electrostatic interactions within cationic lipid/DNA lamellar complexes, Chem. Phys. Lett. 400 (2004) 314–319.
[51] G. Caracciolo, D. Pozzi, A. Amici, H. Amenitsch, Universality of DNA adsorption behavior on the cationic membranes of nanolipoplexes, J. Phys. Chem. B 114 (2010) 2028–2032.
[52] C. Marchini, M. Montani, A. Amici, D. Pozzi, R. Caminiti, G. Caracciolo, Surface area of lipid membranes regulates the DNA-binding capacity of cationic liposomes, Appl. Phys. Lett. 94 (2009) 033903.
[53] M. Muñoz-Úbeda, S.K. Misra, A.L. Barrán-Berdón, C. Aicart-Ramos, M.B. Sierra, J. Biswas, P. Kondaiah, E. Junquera, S. Bhattacharya, E. Aicart, Why is less cationic lipid required to prepare lipoplexes from plasmid DNA than linear DNA in gene therapy? J. Am. Chem. Soc. 133 (2011) 18014–18017.
[54] G. Khelashvili, M. Rappolt, S.W. Chiu, G. Pabst, D. Harries, Impact of sterol tilt on membrane bending rigidity in cholesterol and 7DHC-containing DMPC membranes, Soft Matter 7 (2011) 10299–10312.
[55] S. Perutkova, M. Daniel, M. Rappolt, G. Pabst, G. Dolinar, V. Kralj-Iglic, A. Iglic, Elastic deformations in hexagonal phases studied by small angle X-ray diffraction and simulations, Phys. Chem. Chem. Phys. 13 (2011) 3100–3107.
[56] A. Zidovska, H.M. Evans, A. Ahmad, K.K. Ewert, C.R. Safinya, The role of cholesterol and structurally related molecules in enhancing transfection of cationic liposome–DNA complexes, J. Phys. Chem. B 113 (2009) 5208–5216.
[57] X.X. Zhang, P.G. Allen, M. Grinstaff, Macropinocytosis is the major pathway responsible for DNA transfection in CHO cells by a charge-reversal amphiphile, Mol. Pharm. 8 (2011) 758–766.
[58] J.J. Lu, R. Langer, J. Chen, A novel mechanism is involved in cationic lipid-mediated functional siRNA delivery, Mol. Pharm. 6 (2010) 763–771.
[59] A. Ortiz, J.A. Killian, A.J. Verkleij, J. Wilschut, Membrane fusion and the lamellar-to-inverted-hexagonal phase transition in cardiolipin vesicle systems induced by divalent cations, Biophys. J. 77 (1999) 2003–2014.
[60] M.C. de Lima, S. Simões, P. Pires, R. Gaspar, V. Slepushkin, N. Düzgünes, Gene delivery mediated by cationic liposomes: from biophysical aspects to enhancement of transfection, Mol. Membr. Biol. 16 (1999) 103–109.
[61] D. Top, R. de Antueno, J. Salsman, J. Corcoran, J. Mader, D. Hoskin, A. Touhami, M.H. Jericho, R. Duncan, Liposome reconstitution of a minimal protein-mediated membrane fusion machine, EMBO J. 24 (2005) 2980–2988.
[62] Y.A. Goryacheva, O.M. Vekshina, V.A. Yashin, Y.A. Kim, Fusion and endocytosis of anionic liposomes with Ehrlich ascitic carcinoma cells, Bull. Exp. Biol. Med. 140 (2005) 733–735.
[63] S. Resina, P. Prevot, A.R. Thierry, Physico-chemical characteristics of lipoplexes influence cell uptake mechanisms and transfection efficacy, PLoS One 4 (2009) e6058.
[64] Cardarelli, D. Pozzi, A. Bifone, C. Marchini, G. Caracciolo, Cholesterol-dependent macropinocytosis and endosomal escape control the transfection efficiency of lipoplexes in CHO living cells, Mol. Pharm. DOI: http://dx.doi.org/10.1021/mp200374e.
[65] O. Le Bihan, R. Chèvre, S. Mornet, B. Garnier, B. Pitard, O. Lambert, Probing the in vitro mechanism of action of cationic lipid/DNA lipoplexes at a nanometric scale, Nucleic Acids Res. 39 (2011) 1595–1609.
[66] A. Manosroi, K. Thathang, J. Manosroi, R.G. Werner, R. Schubert, R. Peschka-Süss, Expression of luciferase plasmid (pCMVLuc) entrapped in DPPC/cholesterol/DDAB liposomes in HeLa cell lines, J. Liposome Res. 19 (2009) 131–140.
[67] H.R. Samadikhah, A. Majidi, M. Nikkhah, S. Hosseinkhani, Preparation, characterization, and efficient transfection of cationic liposomes and nanomagnetic cationic liposomes, Int. J. Nanomedicine 6 (2011) 2275–2283.
[68] Q.D. Huang, W.J. Ou, H. Chen, Z.H. Feng, J.Y. Wang, J. Zhang, W. Zhu, X.Q. Yu, Novel cationic lipids possessing protonated cyclen and imidazolium salt for gene delivery, Eur. J. Pharm. Biopharm. 78 (2011) 326–335.
[69] J. Biswas, A. Bajaj, S. Bhattacharya, Membranes of cationic gemini lipids based on cholesterol with hydroxyl headgroups and their interactions with DNA and phospholipid, J. Phys. Chem. B 115 (2011) 478–486.
[70] R.U. Islam, J. Hean, W.A. van Otterlo, C.B. de Koning, P. Arbuthnot, Efficient nucleic acid transduction with lipoplexes containing novel piperazine- and polyamine-conjugated cholesterol derivatives, Bioorg. Med. Chem. Lett. 19 (2009) 100–103.
[71] Y. Zhang, E.L. Bradshaw-Pierce, A. Delille, D.L. Gustafson, T.J. Anchordoquy, In vivo comparative study of lipid/DNA complexes with different in vitro serum stability: effects on biodistribution and tumor accumulation, J. Pharm. Sci. 97 (2008) 237–250.
[72] S. Duarte, H. Faneca, M.C. de Lima, Non-covalent association of folate to lipoplexes: a promising strategy to improve gene delivery in the presence of serum, J. Control. Release 149 (2011) 264–272.
[73] T. dos Santos, J. Varela, I. Lynch, A. Salvati, K.A. Dawson, Quantitative assessment of the comparative nanoparticle-uptake efficiency of a range of cell lines, Small 7 (2011) 3341–3349.
[74] R. Koynova, L. Wang, Y. Tarahovsky, R.C. MacDonald, Lipid phase control of DNA delivery, Bioconjug. Chem. 16 (2005) 1335–1339.
[75] R. Koynova, L. Wang, R.C. MacDonald, An intracellular lamellar–nonlamellar phase transition rationalizes the superior performance of some cationic lipid transfection agents, Proc. Natl. Acad. Sci. U. S. A. 103 (2006) 14373–14378.
[76] R. Koynova, Y. Tarahovsky, L. Wang, R.C. MacDonald, Lipoplex formulation of superior efficacy exhibits high surface activity and fusogenicity, and readily releases DNA, Biochim. Biophys. Acta 1768 (2007) 375–386.
[77] R. Koynova, Lipid phases eye of lipofection: cationic phosphatidylcholine derivatives as efficient DNA carriers for gene delivery, Lipids Insights 2 (2008) 41–59.
[78] J.N. Israelachvili, Intermolecular and Surface Forces, 2nd ed. Academic Press, London, 1992.
[79] X. Ming, K. Sato, R.L. Juliano, Unconventional internalization mechanisms underlying functional delivery of antisense oligonucleotides via cationic lipoplexes and polyplexes, J. Control. Release 153 (2011) 83–92.
[80] Z. Chen, R.P. Rand, The influence of cholesterol on phospholipid membrane curvature and bending elasticity, Biophys. J. 73 (1997) 267–276.
[81] S. Aeffner, T. Reusch, B. Weinhausen, T. Salditt, Membrane fusion intermediates and the effect of cholesterol: an in-house X-ray scattering study, Eur. Phys. J. E 30 (2009) 205–214.
[82] B.G. Tenchov, R.C. MacDonald, D.P. Siegel, Cubic phases in phosphatidylcholine–cholesterol mixtures: cholesterol as membrane "fusogen", Biophys. J. 91 (2006) 2508–2516.
[83] T. Phalen, M. Kielian, Cholesterol is required for infection by Semliki Forest virus, J. Cell Biol. 112 (1991) 615–623.
[84] Z. Liao, L.M. Cimakasky, R. Hampton, D.H. Nguyen, J.E.K. Hildreth, Lipid rafts and HIV pathogenesis: host membrane cholesterol is required for infection by HIV type 1, AIDS Res. Hum. Retroviruses 17 (2001) 1009–1019.
[85] M.A. Churchward, T. Rogasevskaia, J. Höfgren, J. Bau, J.R. Coorssen, Cholesterol facilitates the native mechanism of Ca^{2+}-triggered membrane fusion, J. Cell Sci. 118 (2005) 4833–4848.
[86] J.P. Laliberte, A.S. Weisberg, B. Moss, The membrane fusion step of vaccinia virus entry is cooperatively mediated by multiple viral proteins and host cell components, PLoS Pathog. 7 (2011) e1002446.
[87] S.J. Tucker, D. McClelland, M. Jaspars, K. Sepcić, D.J. MacEwan, R.H. Scott, The influence of alkyl pyridinium sponge toxins on membrane properties, cytotoxicity, transfection and protein expression in mammalian cells, Biochim. Biophys. Acta 1614 (2003) 171–181.
[88] M.A. Ilies, B.H. Johnson, F. Makori, A. Miller, W.A. Seitz, E.B. Thompson, A.T. Balaban, Pyridinium cationic lipids in gene delivery: an in vitro and in vivo comparison of transfection efficiency versus a tetraalkylammonium congener, Arch. Biochem. Biophys. 435 (2005) 217–226.
[89] J.A. Kim, C. Åberg, A. Salvati, K.A. Dawson, Role of cell cycle on the cellular uptake and dilution of nanoparticles in a cell population, Nat. Nanotechnol. 7 (2011) 62–68.
[90] A. Salvati, C. Åberg, T. dos Santos, J. Varela, P. Pinto, I. Lynch, K.A. Dawson, Experimental and theoretical comparison of intracellular import of polymeric nanoparticles and small molecules: toward models of uptake kinetics, Nanomedicine 7 (2011) 818–826.